International Journal of Pharmaceutics 393 (2010) 167–175

Contents lists available at ScienceDirect

International Journal of Pharmaceutics

journal homepage: www.elsevier.com/locate/ijpharm

Pharmaceutical Nanotechnology

Optimization and physicochemical characterization of a triamcinolone acetonide-loaded NLC for ocular antiangiogenic applications

J. Araújo[a], E. Gonzalez-Mira[a], M.A. Egea[a], M.L. Garcia[a], E.B. Souto[b,c,*]

[a] Department of Physical Chemistry, Institute of Nanoscience and Nanotechnology, Faculty of Pharmacy, University of Barcelona, Av. Joan XXIII s/n, 08028 Barcelona, Spain
[b] Institute of Biotechnology and Bioengineering, Centre of Genetics and Biotechnology University of Trás-os-Montes and Alto Douro (IBB/CGB-UTAD), P.O. Box 1013, 5000-801 Vila-Real, Portugal
[c] Department of Pharmaceutical Technology, Faculty of Health Sciences, Fernando Pessoa University, Rua Carlos da Maia, Nr. 296, Office S.1, P-4200-150 Porto, Portugal

ARTICLE INFO

Article history:
Received 27 November 2009
Received in revised form 9 March 2010
Accepted 10 March 2010
Available online 31 March 2010

Keywords:
Triamcinolone acetonide
Nanostructured lipid carriers
NLC
Factorial design
Angiogenics

ABSTRACT

The purpose of this study was to develop a novel nanostructured lipid carrier (NLC) for the intravitreal-targeting delivery of triamcinolone acetonide (TA) by direct ocular instillation. A five-level central composite rotable design was used to study the influence of four different variables on the physicochemical characteristics of NLCs. The analysis of variance (ANOVA) statistical test was used to assess the optimization of NLC production parameters. The systems were produced by high pressure homogenization using Precirol®ATO5 and Squalene® as solid and liquid lipids respectively, and Lutrol®F68 as surfactant. Homogenization at 600 bar for 3 cycles of the optimized formulation resulted in the production of small NLC (mean diameter < 200 nm) with a homogeneous particle size distribution (polydispersity index (PI) ~ 0.1), of negatively charged surface (~|45| mV) and high entrapment efficiency (~95%). Surface morphology was assessed by SEM which revealed fairly spherical shape. DSC, WAXS and FT-IR analyses confirmed that TA was mostly entrapped into the NLC, characterized by an amorphous matrix. *In vivo* Draize test showed no signs of ocular toxicity.

1. Introduction

For decades, corticosteroids have been used in ophthalmology to suppress intraocular inflammation and to reduce extravasation from leaking blood vessels. Intravitreal injections of ophthalmic suspensions containing triamcinolone acetonide (TA), of several brands (e.g. Kenalog®, Tricinolon®, Flutex® and Kenacort®) have become increasingly popular for treating a broad spectrum of retinal diseases (Jonas, 2006). These may offer a possible adjunctive treatment for several clinical conditions namely: (i) intraocular edematous and neovascular disorders e.g. diffuse diabetic macular edema, branch retinal vein occlusion, central retinal vein occlusion and pseudophakic cystoid macular edema (Sung and Jae, 2008; Scott et al., 2003); (ii) to increase visual acuity and decrease intraocular inflammation in eyes with various types of non-infectious uveitis (Degenring and Jonas, 2003); (iii) as angiostatic therapy in eyes with iris neovascularization and proliferative ischemic retinopathies (Jonas et al., 2005); (iv) alone or in combination with photodynamic therapy for exudative age-related macular degeneration (Piermarocchi et al., 2008). The efficacy of TA injections involves multiple mechanisms, including inhibition of phospholipase A2 by lipocortins, increase of tight junction integrity and downregulation of the effects of vascular endothelial growth factor (Mansoor et al., 2009). However, while the drug is effective, the drug delivery system is not ideal. Complications of intravitreal TA therapy include secondary ocular hypertension, cataractogenesis, postoperative infectious and non-infectious endophthalmitis and pseudo-endophthalmitis (Jonas, 2005). Besides, any intraocular injection carries the risk of vision loss from infection, retinal detachment or haemorrhage.

Novel and more efficient delivery systems are being sought, but due to the poor solubility in water and physiologically acceptable organic solvents, the development of TA dosage forms is limited, and most available nanoparticle systems suffer from a low drug content (Valero et al., 1996).

Colloidal drug carriers offer a number of potential advantages as delivery systems for topical route of administration, including: (i) better bioavailability for poorly soluble drugs, (ii) the use of physiological lipids, (iii) the avoidance of organic solvents in the preparation process, (iv) a wide potential application spectrum, (v) improved bioavailability, (vi) protection of sensitive drug molecules from the environment and (vii) a targeted and controlled release characteristics, reducing or preventing side effects being

* Corresponding author at: Faculty of Health Sciences, Fernando Pessoa University, Rua Carlos da Maia, Nr. 296, Office S.1, P-4200-150 Porto, Portugal, Tel.: +351 225 074630; fax: +351 225 074637.
E-mail address: eliana@ufp.edu.pt (E.B. Souto).

0378-5173/$ – see front matter © 2010 Elsevier B.V. All rights reserved.
doi:10.1016/j.ijpharm.2010.03.034

therefore ideal for long-term use drugs (Müller et al., 2000; Souto and Müller, 2006).

Nanostructured lipid carriers (NLC), a new generation of lipid nanoparticles, consist of solid lipid matrices with spatially incompatible liquid lipids resulting in a structure with more imperfections in crystal to accommodate the drug (Souto et al., 2004). They combine the advantages of SLN and overcome their limitations, namely, limited drug loading, risk of gelation and drug leakage during storage caused by lipid polymorphism (Müller et al., 2002).

Previous works have shown the encapsulation of triamcinolone and its derivates into liposomes (Clares et al., 2009), polymeric nanoparticles (Da Silva-Junior et al., 2009) and SLN for transdermal iontophoretic delivery (Liu et al., 2008). However, there are missing studies for NLC and intraocular delivery. Therefore, to reduce the systemic adverse effects of steroids, to have simultaneously high concentrations of the drug at the site of action and for a prolonged time, and to avoid the risks involved in intravitreal injection, attempts have been made to design an innovative TA delivery system for ophthalmic application. A number of peer-review papers have discussed the delivery of drugs to the posterior segment of the eye via topical administration (Sahoo et al., 2008; Duvvuri et al., 2003; Mainardes et al., 2005). From a recent study by Hironaka et al. (2009), these authors claimed the advantages of liposome-based eye drops to potentially target drugs to the posterior segment. The authors have used a fluorescent dye (as hydrophobic model drug) to tackle the in situ behaviour of submicron-sized colloidal carriers based rigid structures. While delivery by means of drug solution shows some shortcomings, the possibility of nanoparticles to reach the posterior tissues and deliver drugs at targeted sites at effective therapeutic concentration has been envisaged and proposed by some authors (Nagarwal et al., 2009). The present paper reports the optimization of an NLC formulation by means of factorial design approaches to ultimately develop a solid, low sized TA-loaded NLC for ocular instillation.

2. Experimental

2.1. Materials

Precirol® ATO5 (PRE), a mixture of mono-, di- and triglycerides of palmitic acid (C_{16}) and stearic acid (C_{18}), was a gift from Gattefosse S.A. (Saint-Priest, France) and Lutrol® F68 (LUT), a hydrophilic block copolymer of ethylene oxide and propylene oxide, from BASF (Barcelona, Spain). Triamcinolone acetonide (TA) and Squalene® (SQ), an unsaturated aliphatic hydrocarbon, were purchased from Sigma (St. Louis, EUA). Double distilled water was used after filtration in a Millipore® system home supplied. All other reagents were of analytical grade.

2.2. Methods

2.2.1. Production of NLC

In the present work, two chemically different lipids were selected from a list of solid and liquid lipids build for lipid screening tests. The rationale was to select those lipids that could better dissolve TA, being simultaneously suitable for ophthalmic use. LUT was chosen as wetting agent. NLC were prepared by high pressure homogenization (HPH) described by Müller and Lucks (1996). Briefly, the lipid phase containing TA, PRE and SQ was heated up to 80 °C to melt the lipids and to obtain a homogeneous lipid solution where 0.025% TA is dissolved. The hot lipid phase was dispersed in the surfactant (LUT) solution heated at the same temperature, by high-speed stirring using Ultra Turrax T-10 (IKA, Germany) to form a pre-emulsion, which was then passed through a high pressure homogenizer (APV 2000, Denmark). Homogenizer was turned on 30 min before starting the production to allow recirculating hot MilliQ water at 80 °C, under pressure at 600 bar. While processing the samples in APV 2000, the temperature of the homogenization circuit was maintained at 80 ± 0.5 °C by coating the machine with a heater tape. A digital thermometer was placed in the sample collecting deposit, to avoid risk of boiling. Finally, the resulting hot o/w nanoemulsion was cooled to 4 °C, recrystallizing the lipid and forming the NLC.

Table 1
Parameters evaluated in preliminary experiments.

Parameter			
UTt (s)	30	60	90
Cycles	3	5	7
Pressure (bar)	500	750	1000

To assess the optimal conditions of the technical procedure, a total of 27 preliminary experiments were undertaken varying 1 of 3 parameters at a time, as described in Table 1, namely, the Ultra Turrax time (UTt) in the pre-emulsion, the number of cycles and pressure upon HPH. Since the influence of each parameter on the physicochemical properties of NLC was not previously assessed during preliminary studies, the experimental concentrations were set based on literature search, as follows: 7% PRE, 3% SQ, 3% LUT and 87% Water.

2.2.2. Factorial design

A four factor, five-level central composite rotatable design 2^4+ principal (Box et al., 1978) was selected to study the effect of 4 independent variables, lipid concentration (X_1), solid lipid concentration in the total lipid phase (X_2), surfactant concentration (X_3) and drug concentration (X_4), on the mean particle size (measured either by photon correlation spectroscopy or laser diffraction), polydispersity index (PI), zeta potential (ZP), and entrapment efficiency (EE) of TA-NLC. An initial 2^4 full factorial design was created, providing the upper (+1) and lower (−1) level values for each evaluated parameter (X_1–X_4) (Table 2). A total of 26 experiments were required (factorial points, Table 3). Effects and interactions between factors were calculated. To determine the effect of a particular factor x (Ex), the following equation was applied:

$$Ex = \frac{\sum x(+) - \sum x(-)}{n/2}$$

where Σx (+) is the sum of the factors at their highest level (+1), Σx (−) is the sum of the factors at their lowest level (−1), and $n/2$ is the half of the number of measurements used in the calculation.

The 2^4 full factorial design was expanded to a central composite. The advantage of this method is that by adding just 10 "star" points (8 axial points and 2 replicated centre points, Table 3) to the initial factorial design, extra levels for the four factors are created resulting in five levels for each one (Table 2).

The studied experimental responses were the results of the individual influence and the interactions of the 4 independent variables. The responses were therefore modelled by the following

Table 2
Independent variables and their correspondence between real and five-level values in experimental design. %L, concentration of lipid phase; %PRE/L, concentration of Precirol® with regard to the lipid phase; %LUT, concentration of Lutrol® F68; %TA, concentration of triamcinolone acetonide.

Parameter		−1.68	−1	0	+1	+1.68
X_1	%L	6	8	10	12	14
X_2	%PRE/L	55	65	75	85	95
X_3	%LUT	0	1	2	3	4
X_4	%TA	0	0.05	0.1	0.15	0.2

Table 3
Coded level of factors and measured responses of the evaluated parameters. %L, concentration of lipid phase; %PRE/L, concentration of Precirol® with regard to the lipid phase; %LUT, concentration of Lutrol®F68; %TA, concentration of triamcinolone acetonide.

Coded levels of factors					Measured responses				
	%L	%PRE/L	%LUT	%TA	PCS (nm) ± SD	LD 90 (nm) ± SD	ZP (mV) ± SD	PI ± SD	EE (%) ± SD
	Factorial points								
1	−1	−1	−1	−1	207.20 ± 2.27	279 ± 3.00	−45.60 ± 1.07	0.09 ± 0.03	49.87 ± 0.56
2	1	−1	−1	−1	311.70 ± 2.01	532 ± 16.00	−41.30 ± 0.10	0.20 ± 0.00	45.67 ± 0.28
3	−1	1	−1	−1	231.50 ± 6.40	244 ± 1.00	−43.60 ± 0.66	0.05 ± 0.04	55.54 ± 0.47
4	1	1	−1	−1	327.20 ± 1.36	416 ± 7.00	−45.20 ± 0.40	0.23 ± 0.04	52.85 ± 0.39
5	−1	−1	1	−1	133.70 ± 1.25	180 ± 1.00	−39.00 ± 1.76	0.16 ± 0.02	48.83 ± 0.08
6	1	−1	1	−1	191.60 ± 1.95	227 ± 1.00	−39.00 ± 0.36	0.13 ± 0.01	58.46 ± 0.24
7	−1	1	1	−1	162.60 ± 0.00	188 ± 0.00	−37.40 ± 2.26	0.13 ± 0.01	33.81 ± 0.95
8	1	1	1	−1	230.70 ± 3.51	222 ± 1.00	−37.30 ± 0.76	0.12 ± 0.01	45.98 ± 0.31
9	1	1	1	1	238.60 ± 5.92	228 ± 2.00	−37.50 ± 0.60	0.15 ± 0.02	51.78 ± 0.66
10	−1	1	1	1	167.30 ± 2.21	206 ± 1.00	−30.60 ± 1.38	0.16 ± 0.01	33.98 ± 0.42
11	1	−1	1	1	205.90 ± 3.51	237 ± 1.00	−42.00 ± 0.17	0.15 ± 0.02	47.74 ± 0.76
12	−1	−1	1	1	143.70 ± 1.07	187 ± 0.00	−36.00 ± 0.35	0.16 ± 0.01	57.59 ± 0.13
13	1	1	−1	1	–	659 ± 31.00	−39.10 ± 0.53	–	49.79 ± 0.55
14	−1	1	−1	1	239.50 ± 1.76	259 ± 1.00	−42.20 ± 0.59	0.17 ± 0.02	67.62 ± 0.20
15	1	−1	−1	1	428.10 ± 15.53	549 ± 12.00	−40.00 ± 0.58	0.20 ± 0.01	60.61 ± 0.34
16	−1	−1	−1	1	199.20 ± 1.36	239 ± 2.00	−39.50 ± 0.60	0.10 ± 0.01	69.19 ± 0.41
	Axial points								
17	1.68	0	0	0	325.60 ± 3.81	640 ± 23.00	−34.50 ± 0.71	0.16 ± 0.01	28.89 ± 0.91
18	−1.68	0	0	0	145.50 ± 0.61	187 ± 0.00	−35.50 ± 0.32	0.17 ± 0.01	60.20 ± 0.73
19	0	1.68	0	0	222.20 ± 0.61	229 ± 2.00	−29.30 ± 0.32	0.14 ± 0.01	45.30 ± 0.64
20	0	−1.68	0	0	174.30 ± 1.83	211 ± 2.00	−47.50 ± 0.06	0.12 ± 0.02	45.92 ± 0.59
21	0	0	1.68	0	159.50 ± 2.59	201 ± 1.00	−41.10 ± 0.90	0.16 ± 0.01	54.39 ± 0.77
22	0	0	−1.68	0	–	–	–	–	–
23	0	0	0	1.68	215.70 ± 2.40	226 ± 1.00	−45.60 ± 1.14	0.11 ± 0.02	46.25 ± 0.00
24	0	0	0	−1.68	–	–	–	–	–
	Centre points								
25	0	0	0	0	206.70 ± 1.46	225 ± 1.00	−44.30 ± 0.32	0.11 ± 0.02	38.97 ± 0.24
26	0	0	0	0	209.00 ± 2.55	232 ± 2.00	−42.03 ± 0.57	0.12 ± 0.00	40.77 ± 0.78

polynomial model:

$$Y = \beta_0 + \beta_1 X_1 + \beta_2 X_2 + \beta_3 X_3 + \beta_4 X_4 + \beta_{11} X_1^2 + \beta_{22} X_2^2 + \beta_{33} X_3^2 + \beta_{44} X_4^2 + \beta_{12} X_1 X_2 + \beta_{13} X_1 X_3 + \beta_{14} X_1 X_4 + \beta_{23} X_2 X_3 + \beta_{24} X_2 X_4 + \beta_{34} X_3 X_4$$

where Y is the measured response, β_0 the intercept term, β_i's (for $i = 1$–4) are the linear effects, β_{ii}'s the quadratic effects, β_{ij}'s (for $i,j = 1$–4, $i < j$) the interaction between the ith and jth variables. To perform the statistical data analysis, the Statgraphics centurion software was employed and analysis of variance (ANOVA) was able to determine the significance of the factors and interactions between them.

2.3. Physicochemical characterization

2.3.1. Mean particle size and zeta potential analysis

The mean particle size (size), polydispersity index (PI) and zeta potential (ZP) were determined by photon correlation spectroscopy (PCS) with a Zetasizer Nano ZS (Malvern Instruments, UK) at 25 °C using disposable polystyrene cells and disposable plain folded capillary zeta cells, respectively, after appropriate dilution with ultra-purified water. For size measurements of lipid nanoparticle dispersions refractive index was set as RI = 1.456 (abs = 0.01) (Keck and Muller, 2008). The laser diffraction (LD) particle size analysis was performed by a Mastersizer Hydro 2000MU (Malvern Instruments, UK). Data was evaluated using the volume distribution method to detect even few large particles and characterization parameters were LD 50 and LD 90 (i.e., a diameter LD 90 of 1 μm means that 90% of all particles have 1 μm or less).

2.3.2. Morphological studies

The NLC were examined morphologically in a field emission Hitachi S-4100 Scanning Electron Microscope (Hitachi, Japan). Samples were prepared by placing a droplet onto an aluminium specimen stub, dried overnight and sputter coated with gold prior to imaging.

2.3.3. Entrapment efficiency

Assessment of drug location and amount entrapped in NLC is of paramount importance, since it influences the release profile. The entrapment efficiency (EE) of TA in NLC was assessed indirectly, determining the free TA (non-entrapped) by reverse-phase high-performance liquid chromatography (RP-HPLC), using a modification of the USP method (Valero et al., 1996), and applying the following equation:

$$\text{EE}(\%) = \frac{\text{Total amount of TA} - \text{Free TA}}{\text{Total amount of TA}} \times 100$$

Free TA was removed by filtration/centrifugation technique using centrifugal filter devices Ultracel YM-100 (Amicon® Millipore Corporation, Bedford, MA) at 3000 rpm for 15 min (Sigma 301 K centrifuge, Spain). Prior to filtration/centrifugation, each sample was diluted with MilliQ water (1:20) to avoid deposition of free TA (possibly crystallized in the aqueous phase) onto the NLC surface and thus measured as encapsulated. If previously diluting the samples, all free TA passes through the filter and is adequately quantified by RP-HPLC. The RP-HPLC system consisted of a Waters 1525 pump (Waters, Milford, MA) with a UV–vis 2487 detector (Waters) set at 254 nm. A reverse-phase column (Hyperpack® ODS 5 μm, 10 × 0.46) with a flow rate of 1 mL/min was used. The mobile phase consisted of acetonitrile:methanol:water (30:10:60).

2.3.4. Differential scanning calorimetry (DSC)

DSC analysis was performed using a Mettler TA 4000 system (Greifensee, Switzerland) equipped with a refrigerated cooling system. The instrument was calibrated with indium. Bulk materials, lipid mixtures and NLC (1–2 mg lipid) were put into aluminium

pans. The thermal analysis profiles were obtained as the temperature was increased from 25 °C to 80 °C or to 320 °C for bulk TA at a rate of 5 °C/min under nitrogen atmosphere and using an empty pan as reference. DSC thermograms were recorded for bulk TA, bulk PRE, mixture of PRE:SQ (70:30) with and without TA, and for TA-free and TA-loaded NLC stored at different temperatures. Bulk PRE and lipid mixtures were heated at 80 °C and recrystallized to give TA the possibility to dissolve, if required, and to imitate the production process of NLC.

2.3.5. Wide angle X-ray scattering (WAXS)

WAXS diffractograms were captured on a PANalytical X'Pert PRO power diffractometer (Almelo, The Netherlands) with copper anode (Cu-Kα radiation, λ = 1.5418 nm) and X'Celerator detector. The diffractograms were measured at angles 2θ = 15–40° with step of 0.017° and count time of 50 s.

WAXS analysis of TA, PRE and LUT was performed as powders, lipid mixtures were performed after melting the lipid, to mimic the thermal treatment used in HPH method, whereas NLC dispersions were analysed directly without further treatment.

2.3.6. Fourier transform infrared (FT-IR) spectroscopy

IR-spectra of TA and the optimized formulation were obtained on a ABB FTLA2000 IR-spectrophotometer (Zurich, Switzerland). Potassium bromide discs containing the samples (1%, w/w) were prepared prior to analysis.

2.4. In vivo Draize test

Since tears have limited buffering capacity and irritation associated with the instillation of hypo- or hypertonic suspensions may cause reflex blinking (Thomas et al., 1997), sample osmolarity was adjusted with glycerine to 310 mOs/kg, evaluated by freeze-drying point measurements on a Fiske osmometer, and pH with 0.1N NaOH to 7.4. To test the ocular tolerance to TA-NLC *in vivo*, an updated version of the Draize eye test was undertaken (Kay and Calandra (1962)). Three male albino New Zealand rabbits weighing 2.0–2.5 kg were used. Animals received 50 μL of the optimized 0.025% TA-NLC formulation in the conjunctival sac of the right eye. The contralateral eye was used as control and received no treatment. Readings were recorded 1 h after application of the test substance, and then after 1, 2, 3, 4 and 7 days. The method provided an overall scoring system for grading the severity of ocular lesions involving the cornea (opacity), iris (inflammation degree), and conjunctiva (congestion, swelling and discharge). The Draize score was determined by visual assessment of changes in these ocular structures. The mean total score (MTS) was calculated as follows:

$$\mathrm{MTS}(\%) = \sum \frac{x_1(n)}{5} + \frac{x_2(n)}{2} - \frac{x_3(n)}{5}$$

where $x_1(n)$, $x_2(n)$, and $x_3(n)$ are the cornea, conjunctiva and iris scores, respectively, being n the number of rabbits included in the ocular tolerance assay. Experiments were performed according to the Association for Research in Vision and Ophthalmology (ARVO) resolution of the use of animals in research, approved by the animal research ethical committee of the University of Barcelona and responded to the normative of directive 214/97, Gencat.

3. Results and discussion

3.1. Characterization and optimization of TA-NLC

In the development of a drug delivery system for ocular administration, the particle size is an important parameter to assess the risk of irritation and discomfort. If the particle induces tearing, a rapid drainage of the instilled dose would occur, decreasing the residence time of drug in the conjunctival sac, and reducing thereafter drug bioavailability (Schoenwald and Stewart, 1980). In addition, particle size distribution also influences the penetration mechanism of topically administered drugs. In general, smaller particles (approx. 100 nm) exhibit higher uptake in comparison to those of larger size (between 800 nm and 1000 nm), depicting therefore higher ability to penetrate across the ocular barriers (Nagarwal et al., 2009). On the other hand, it has also been reported that particles below 20 nm are in the cut-off size for rapid clearance (Amrite and Kompella, 2005).

LUT was chosen as surfactant to stabilize NLC in aqueous suspension due to its non-ionic character, because it does not induce strong ocular irritancy (Benita, 1999) and it is accepted by the regulatory authorities for ocular administration (Mclain, 2008). In addition, its melting point is close to the values reported for PRE, while its HLB value of 29 is sufficiently high to lower the surface tension between the lipid excipients and the dissolution medium (Jannin et al., 2006).

To evaluate the optimum experimental conditions for NLC production by HPH, a total of 27 experiments were performed, producing the same NLC formulation for each independent experiment (Fig. 1). No significant differences were observed on the mean particle size and PI values for all NLC, as evaluated by the statistical ANOVA. In the light of these results, the selected parameters for production of all formulations by HPH were: (i) 30 s of pre-homogenization with Ultra Turrax, (ii) 3 cycles and (iii) 600 bar of pressure.

In the field of pharmaceutical dosage forms, to design a new formulation it is of paramount importance identifying the influ-

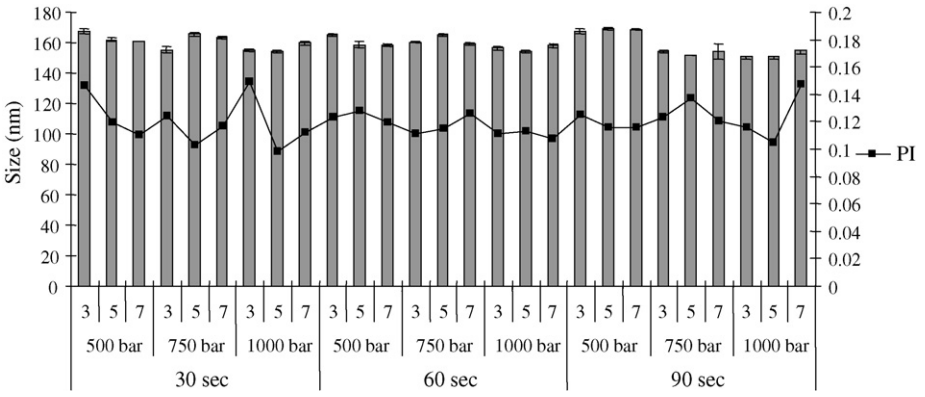

Fig. 1. Mean particle size (nm) and polydispersity index (PI) of the NLC produced in preliminary experiments.

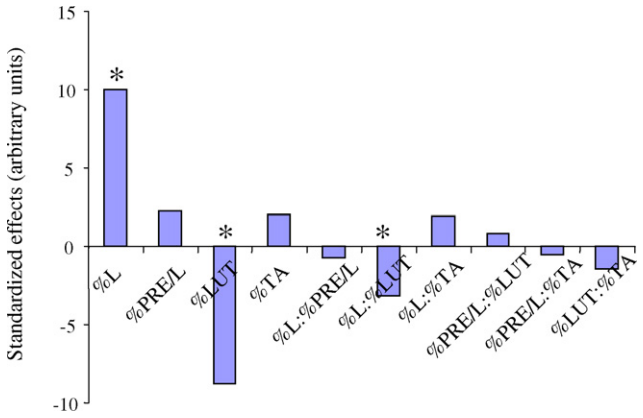

Fig. 2. Evaluation of the standardized effects of the concentration of total lipid phase (%L), concentration of Precirol® with regard to the lipid phase (%PRE/L), concentration of surfactant (%LUT) and of triamcinolone acetonide (%TA), and their interactions on the mean particle size measured by PCS of NLC. *Considered statistically significant for p-value < 0.05.

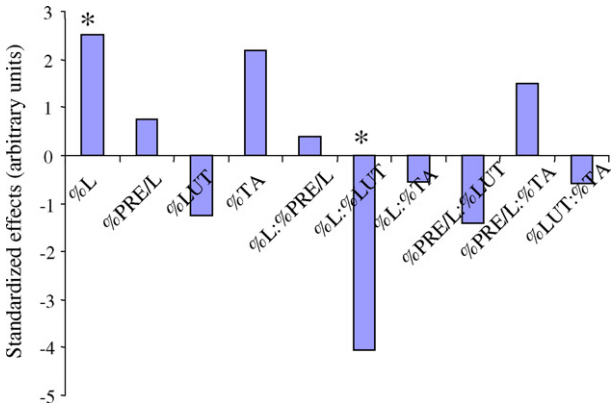

Fig. 4. Evaluation of the standardized effects of the concentration of total lipid phase (%L), concentration of Precirol® with regard to the lipid phase (%PRE/L), concentration of surfactant (%LUT) and of triamcinolone acetonide (%TA), and their interactions on the PI of NLC. *Considered statistically significant for p-value < 0.05.

encing parameters, since these might affect the properties of the final dosage form. The use of experimental designs is nowadays a common method of simultaneously analyzing the influence of different variables on the properties of the drug delivery system being studied (Yang and Zhu, 2002). Using a 2^4 factorial design, and the elected HPH method, the effect of total lipid (L), solid lipid with respect to total lipid (PRE/L), surfactant (LUT) and drug (TA) concentrations on the mean size, PI, ZP, and EE of TA-NLC has been investigated (Table 2). A total of 26 experiments were performed and the results of the designed experiment are shown in Table 3 (factorial points).

To identify the significant effects and interactions, ANOVA statistical tests were performed for each parameter. The results obtained (Fig. 2) indicate that both the lipid phase (%L) and surfactant (%LUT) concentrations had a significant effect on the mean size ($p < 0.05$). This two-factor interaction means that the effect of one factor (%L) is dependent on the level of the other (%LUT), thus interpretation of each isolate factor cannot be made.

To validate the linear mode, 8 axial and 2 centre points were added to the 16 factorial points depicted in Table 3. Quadratic polynomial equations were generated to provide means of evaluating changes in response due to changes in the independent variable levels (%L, %PRE/L, %LUT and %TA). The response surface plot of Figs. 3 and 5 are graphic representation of these equations. From the results obtained of the response surface plot for the interaction between %L and %LUT, an increase of the mean particle size was observed when increasing lipid concentration or decreasing the surfactant. Generally, with a lipid concentration equal or higher than 12%, too viscous samples were produced which could turn into semi-solid when stored at low temperatures (4 °C). A concentration of 9% of total lipid (9 g (lipid mixture)/100 g (NLC)) was then chosen as optimal, since it could maintain the particles within a small sized range. This %L should avoid obtaining too aqueous formulations, and thus potentially considered as nanoemulsions due to the super-cooled status of the lipid matrix. Although not statistically significant, a positive effect for %PRE/L in PCS size could be observed, meaning that increasing %PRE/L a higher tendency to produce larger NLC was observed. These results were also confirmed while measuring NLC size by LD.

Fig. 4 depicts the interaction of parameters with respect to the PI of NLC ranging between 0.09 and 0.23 (Table 3). ANOVA results provide indicate that a significant interaction exists between %L and %LUT, which was previously observed for PCS analysis.

In the response surface plot of Fig. 5, the produced NLC depicted higher PI values when increasing the surfactant concentration above 2%, while maintaining low %L. For the chosen 9% lipid phase concentration the optimal surfactant concentration was set as 2%, since this value could low PI, while keeping NLC within a small sized range.

For the search of an optimal %PRE/L, estimated surface plot contours were designed considering 2%LUT. Results are shown in Fig. 6. The intersection of 9%L with the lowest PI value (0.106) corre-

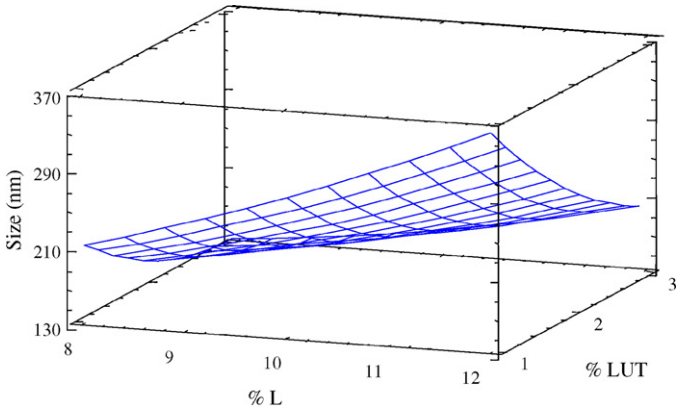

Fig. 3. Response surface plot of the effect of the interaction between lipid phase concentration (%L) and surfactant concentration (%LUT) on the mean particle size (%PRE/L = 70%; %TA = 0.025%), mean size (nm) = 198.73 − 7.49%L − 22.05%LUT + 2.24%L^2 − 10.07%L %LUT + 19.54%LUT^2.

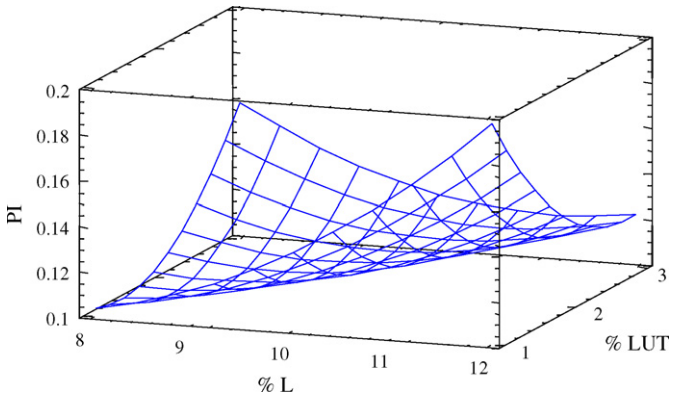

Fig. 5. Response surface plot of the effect of the interaction %L and %LUT (%L:%LUT) on the polydispersity index (%PRE/L = 70%; %TA = 0.025%), PI = 0.14 − 0.04%L + 0.08%LUT + 3.93 × 10^{-3}%L^2 − 0.02%L %LUT + 0.02%LUT^2.

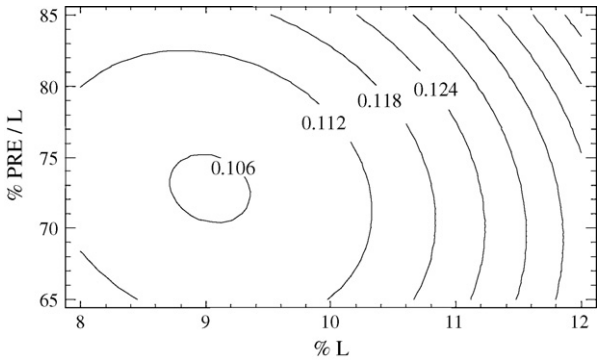

Fig. 6. Response surface contour plot of the effect of the interaction %L and %PRE/L on the PI.

sponded to two possible %PRE/L values (70% versus 75%). Knowing that decreasing %PRE/L is followed by an enhanced tendency to produce smaller particles, a ratio between 70% PRE and 30% SQ was selected.

The ZP represents the electrical charge at the NLC surface, being an indirect measure of the long-term physical stability and mucoadhesion. Higher ZP values, either positively or negatively charged, mean that NLC will have greater long-term stability. The electrostatic repulsion between particles with the same electrical charge avoids the occurrence of aggregation (Feng and Huang, 2001). The obtained ZP results are given in Table 3. Similar to Zhang et al. (2009) who reported the absent quadratic relationship of experimental design parameters with ZP, in the present case no significant differences were observed between samples, showing negatively charged NLC with values ranging from −29.30 mV to −45.60 mV.

With respect to EE, a significant negative effect of %LUT was observed (i.e. EE decreased with increasing %LUT), but no significant interferences between parameters were detected. As the amount of emulsifier increases, the surface of the formed NLC will be too small to adsorb all surfactant molecules, which will result in the formation of micellar solutions. The solubility of TA in the water phase is increased and the drug may suffer partition from the NLC into the formed micelles in the water phase. During the particle washing by ultrafiltration technique preceding EE quantification, TA is lost, reducing therefore the final EE on the surface of the NLC. This phenomenon was also reported previously by Tiyaboonchai et al. (2007). To overcome this loss of drug by micellar solubilisation, 2% LUT is considered an appropriate concentration.

To summarize, an optimal and appropriate NLC formulation for ocular administration (without inducing corneal irritancy, while maintaining small size range) should be composed of 9% lipid phase (70%PRE/30%SQ), 2% LUT, and loaded with 0.025% TA, producing particles with EE of 94.82 ± 1.12% and negative surface charge (ZP = |46.70| ± 0.91 mV).

As reported by Conway et al. (2003), improvement in visual acuity in patients treated with injections of 1 mg TA, required reinjection typically after 4 months. In this way, a daily use instillation of some NLC drops would be a friendlier alternative to overcome multiple injections. Bearing this in mind, a formulation designed to be conveniently administered by incessant frequency shall not be dosed as similar to an extremely high dose designed to be effective for several months with a single administration. In fact, it should be much less. In this way, NLC loaded with a relatively payload (0.025% TA) were produced. After topical administration to the surface of the eye, absorption may occur via systemic pathway (besides corneal and non-corneal pathway) caused by nasolachrymal drainage, and higher doses could lead to serious toxicological and immunological effects.

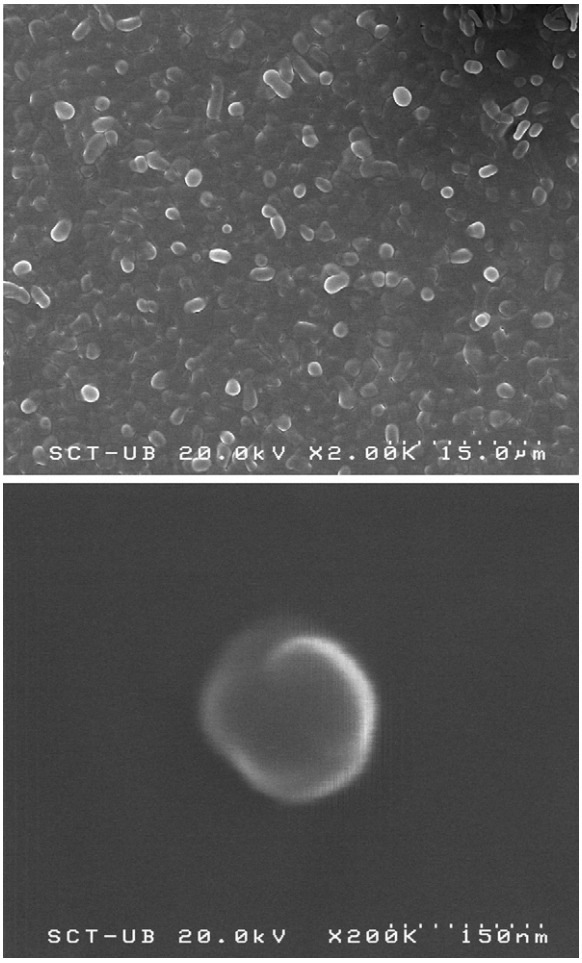

Fig. 7. Scanning electron micrograph of optimized NLC spherical in shape (field overview in (a), with smooth surfaces (b)).

3.2. Morphological studies

SEM analysis (Fig. 7) revealed that optimized NLC were spherical in shape (field overview in Fig. 7(a)) and uniformly distributed. For more detail, their smooth surfaces are depicted in Fig. 7(b). An increase in particle size diameter was observed by SEM being attributed to the presence oil. Nanocompartments of oil within NLC, turn the particles more vulnerable (e.g. easily fusing and degrading) to the preparation process usually required previously to SEM analysis. To verify this hypothesis, NLC were analysed for their mean diameter and size distribution, confirming their small size (PCS = 173.30 ± 0.32, LD 90 = 180.00 ± 2.00 nm) and monodispersed population (PI = 0.10 ± 0.02).

3.3. DSC

It has been reported that lipid molecules show different three-dimensional structures: unstable α, metastable β′, and the most stable the β modification, existing additional intermediate β_i forms, between β′ and β, for mixtures of glycerides (Freitas and Müller, 1999). As shown in Fig. 8(a), the bulk PRE exhibits a sharp endothermic event, ascribing to the melting, around 63.90 °C (minimum). This main peak exhibits an extrapolated onset of ∼58.94 °C, with a small but well defined shoulder at 59 °C attributed to the melting of α polymorphic form. The difference between onset and

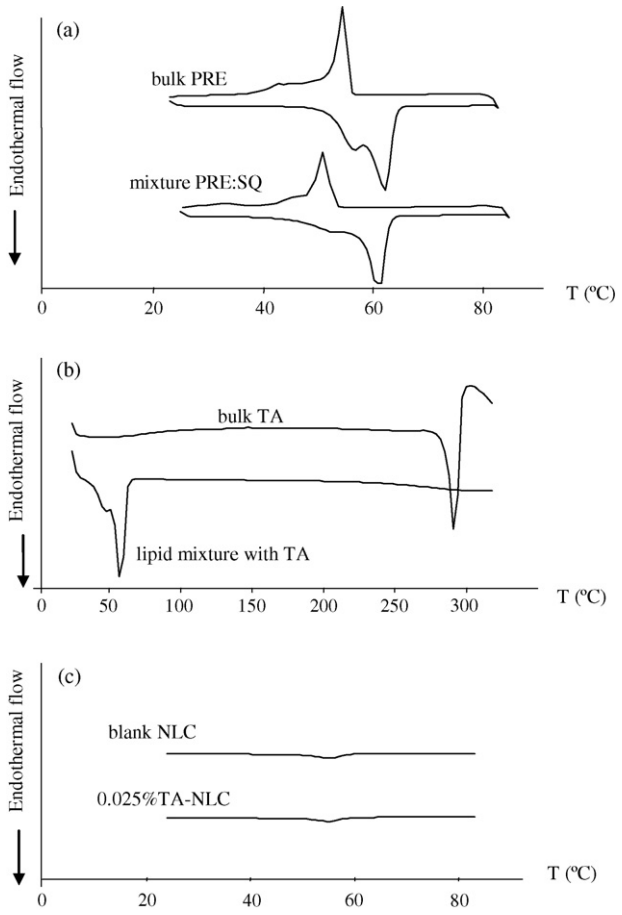

Fig. 8. Differential scanning calorimetry curves of (a) heating and cooling steps of bulk PRE and mixture PRE:SQ; (b) heating step of bulk TA and lipid mixture with drug; (c) heating step of blank and 0.025%TA-loaded NLC.

minimum can be taken as a measure for the width of the peak. Since the diester fraction of the glyceride is predominating (>50%), the main modification in which the bulk PRE crystallizes should be the β′ form (Hagemann and Rothfus, 1993).

The addition of a liquid lipid (SQ) to PRE induced a shift of the melting point to lower temperatures (from 63.90 °C to 61.09 °C) and reduced the enthalpy required to melt the lipid (from 186.55 J/g to 143.29 J/g). As reported by Fang et al. (2008), this energy reduction indicates an interaction of liquid SQ with the crystalline PRE matrix, creating a more massive crystal order disturbance (lattice defects) which could allow enough space to accommodate TA molecules. Likewise, an onset temperature higher than 40 °C was obtained, which is a requirement for the development of NLC for modified drug delivery profiles (Fig. 8(a)).

Since the melting point of TA has been recorded at approximately 293 °C, DSC analysis was run heating the sample from 25 °C to 320 °C. The DSC curve of bulk TA (Fig. 8(b)) showed a melting endotherm at 290 °C followed by decomposition. This result emphasizes the chemical stability of TA under the production conditions applied for the preparation of drug-loaded NLC. DSC analysis of the physical mixture of drug and lipid phase in equivalent concentration as the final optimized formulations, revealed only the melting events of the lipid phase. Since the melting endotherm of TA, was not recorded, the complete solubilisation of TA in the lipid matrix was then anticipated.

Thermal behaviour of lipid materials is dramatically changed from bulk raw materials to lipids processed as nanoparticles. Fig. 8(c) shows a broader endothermic peak occurring at a lower temperature. This melting depression is described in the Thomson equation (derived from the Kelvin equation), being the differences generally ascribed to the interaction of solid lipid with the liquid lipid and surfactant, or simply to the nanometric size of the particles, having then a high specific surface area (Bunjes and Westesen, 2001).

3.4. WAXS

X-ray diffraction data were in good agreement with the results depicted by DSC measurements. The diffraction pattern of TA

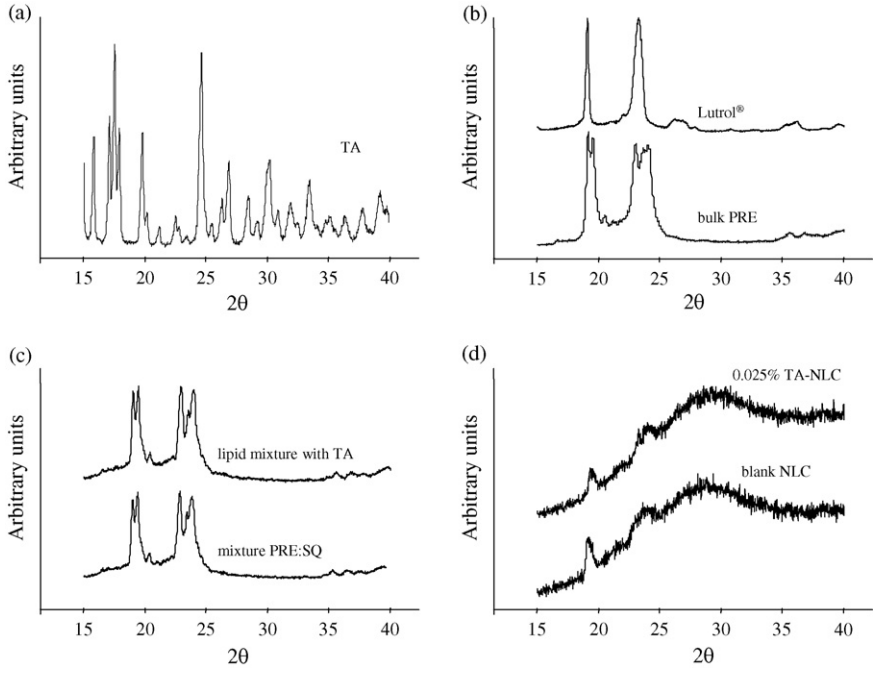

Fig. 9. X-ray diffraction patterns of (a) bulk TA, (b) bulks LUT and PRE, (c) optimized lipid mixture (70%PRE:30%SQ) with and without TA, (d) NLC with and without drug.

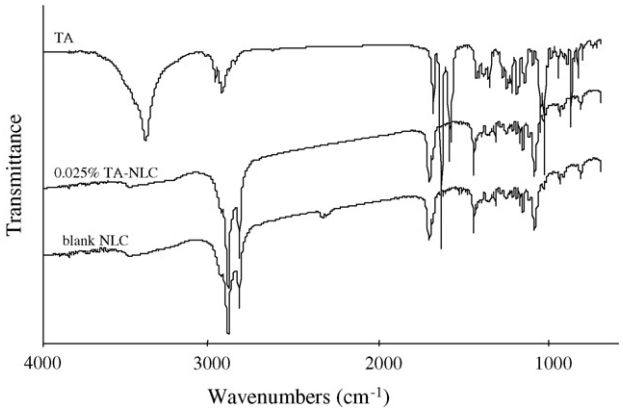

Fig. 10. FT-IR spectra of bulk TA and optimized NLC with and without drug.

(Fig. 9(a)) exhibits two sharp peaks at $2\theta = 17.56^\circ$ and 24.66°, and some peaks of lower intensity, indicating the crystalline nature of TA. The absence of these characteristic reflections in the lipid mixture containing TA (Fig. 9(c)) demonstrates the total solubilisation of drug within the lipid phase. Chemical nature of the lipids plays an important role to obtain adequate drug loading. Lipids that are mixtures of mono-, di-, and triglycerides and containing fatty acids of different chain lengths (e.g. PRE), usually form crystals with many imperfections, offering space to accommodate more drug molecules (Vivek et al., 2007). Main reflections of PRE at $2\theta = 19.49^\circ$, 20.52°, 23.02° and 24.02° (Fig. 9(b)) were also found, in a less ordered crystal state in lipid mixture with SQ (Fig. 9(c)). NLC depicted typical diffraction patterns characterized by a diffuse halo with two broader and much weaker interferences (Fig. 9(d)). Although not shifted, the peaks had a slight reduced intensity in TA-loaded NLC when compared to blank NLC, which may be attributed to the incorporation of TA between parts of the crystal lattice of the lipid, leading to a change in the crystallinity of the TA-loaded NLC.

3.5. FT-IR

The empirical formula of TA is $C_{24}H_{31}FO_6$, structured as 9-fluoro-11β,16α,17,21-tetrahydroxypregna-1,4-diene-3,20-dione 16,17-cyclic acetal with acetone. In FT-IR spectrum (Fig. 10), the characteristic bands observed from the data of TA included the OH group in the range 3650–3200 cm^{-1}, C–H stretching of sp3 and sp2 carbons in the range of 3000 cm^{-1} and 2900 cm^{-1}, C=O in 1775–1650 cm^{-1}, C=C in 1690–1635 cm^{-1}, C–O–C in 1310–1000 cm^{-1} and a strong peak at 1050 cm^{-1} due to stretching vibration of C–F. From FT-IR data of blank and TA-loaded NLC the characteristic absorption bands of axial stretching of sp3 and sp2 carbons were the strongest, followed by the ester group band in the range 1745–1730 cm^{-1}, CH_2–(C=C) deformation vibration at 1440 cm^{-1} and multiple bands related to C–O–C asymmetric stretching vibration (Pretsch et al., 2009). The similar result observed in the spectrum of both NLC formulations, as well as the absence of new bands for TA-NLC, indicates that there was no chemical interaction between the drug and the lipid matrix, being TA only dissolved in the lipid matrix. Similar results were obtained for biodegradable microparticles of poly D,L-lactide-co-glycolide containing triamcinolone (Da Silva-Junior et al., 2009).

3.6. Draize test

The advantages of using lipids as carrier systems for topical administration are related to the physiological and well-tolerated nature of these materials, reducing the risk of toxicological concerns and local irritancy (Souto and Müller, 2009). Topical application of optimized NLC to rabbit eyes showed no sign of toxicity or irritation to the external ocular tissues (MTS = 0 in all cases) after Draize test.

An important factor contributing to ocular irritancy would be the higher polydispersity of the colloidal dispersion. However, in the present case, the surface response design of a truncated set of empirical experiments allowed formulating optimized TA-loaded NLC with low PI and mean size.

In the treatment of physiopathological conditions using ocular drug delivery systems, these should ensure that drug molecules reach the site of action at determined concentrations and within effective therapeutic dosage ranges. The dosage concentration should remain constant throughout the time required to bring about changes in the physiopathological process. With respect to intravitreal TA injections, these dosage forms are far from this premise, since they follow a two-compartment model with an exponential decrease of the drug concentration in the first 4 weeks followed by a more linear decrease during the next months (Kamppeter et al., 2008).

Among the different types of colloidal drug delivery systems, lipid nanoparticles show the ability to target specific tissues and cells, with improved penetration and enhanced drug bioavailability into ocular barriers, increase the therapeutic effectiveness and minimize the undesirable side effects. Furthermore, several commercially available ocular injections have benzyl alcohol in their composition, which is considered potentially toxic. NLC formulations can be easily developed without recurring to organic solvents.

The present work is focused on the optimization of NLC formulations towards their ultimate use of ocular TA delivery. Further investigations must be undertaken to elucidate the pharmacokinetic behaviour of TA from NLC matrix, which might be affected not only by the composition and size, but also by the physiopathology of the eye. Although prospective studies and long-term follow-up period are demanding to achieve consistent outcomes, a novel hypothesis has been here reported to overcome the major shortcomings of drug delivery into the posterior segment by ocular administration.

4. Conclusions

Although studies reporting the ocular penetration of colloidal carriers are lacking, several attempts are being undertaken to justify the enhanced drug penetration, distribution and bioavailability observed by ocular nanoparticle instillations. If a patient is supine and a large drop is allowed to flood the interpalpebral space, the fluid can fall under gravity and distend the cul-the-sac, giving the drug the opportunity to penetrate into the posterior sclera and orbit (Maurice, 2002). Drug penetration and distribution into the posterior tissues of the eye may occur by several pathways, namely, (i) diffusion into the iris root and subsequently into the posterior chamber aqueous humour and into the posterior tissues, (ii) direct entry through the pars plana, (iii) diffusion across the sclera followed by penetration of Bruch's membrane and the retinal pigmented epithelium, and (iv) finally to a lesser extent, absorption into the systemic circulation either through the conjunctival vessels or via nasolachrymal duct and gain systemic access to the retinal vessels (Hughes et al., 2005).

To accomplish the demand for efficient drug delivery systems that may target noninvasively the posterior segment diseases of the eye, attempts have been made to develop submicron-sized colloidal carriers with rigid structures as potential carriers to accomplish this goal (Hironaka et al., 2009). Here, the particle size plays a relevant role. In the present work, a factorial design approach to develop optimized lipid nanoparticles (of mean size 100–300 nm, high ZP and low PI) was reported towards the successful production of TA-

loaded NLC for ocular administration. The optimal physicochemical properties of NLC could be previously settled by varying the processing parameters, and studying the interactions of the influencing factors. Mathematical analysis of these empirical data showed that the optimal formulation should be composed of 9% lipid phase, (based on 70% PRE and 30% SQ), and 2% LUT. A TA concentration of 0.025% was maintained entrapped and solubilised in the lipid matrix of NLC reaching approx. 95% EE. Loading NLC with TA, matrix crystallinity decreased, being the selected lipids suitable materials for TA foreseeing a good long-term physicochemical stability.

The optimized TA-loaded NLC developed by surface response design did not show any irritancy level being therefore a promising effective system for delivery and controlled release of TA with reduced toxicity. The possibility to develop a marketed product based on lipid nanoparticles for a daily drug instillation is still opened to ultimately increase patient's compliance. Further studies are being undertaken to follow up the systems' long-term stability and the in vitro/*in vivo* TA permeation profiles.

Acknowledgment

The authors wish to acknowledge the sponsorship of the Spanish-Portuguese Integrated Actions (ref: HP2008-0015).

References

Amrite, A.C., Kompella, U.B., 2005. Size-dependent disposition of nanoparticles and microparticles following subconjunctival administration. J. Pharm. Pharmacol. 57, 1555–1563.

Benita, S., 1999. Prevention of topical and ocular oxidative stress by positively charged submicron emulsion. Biomed. Pharmacother. 53, 193–206.

Box, G.E.P., Hunter, W.G., Stuart Hunter, J., 1978. Statistics for Experimenters: An Introduction to Design, Data Analysis and Model Building. Wiley Series in Probability and Mathematical Statistics, John Wiley & Sons Publishers.

Bunjes, H., Westesen, K., 2001. Influences of colloidal state on physical properties of solid fats. In: N. Garti, K.S.E. (Ed.), Processes in Fats and Lipid Systems. Marcel Dekker Inc., New York.

Clares, B., Gallardo, V., Medina, M.M., Ruiz, M., 2009. Multilamellar liposomes of triamcinolone acetonide: preparation, stability, and characterization. J. Liposome Res. 19, 197–206.

Conway, M.D., Canakis, C., Livir-Rallatos, C., Peyman, G.A., 2003. Intravitreal triamcinolone acetonide for refractory chronic pseudophakic cystoid macular edema. J. Cataract Refract. Surg. 29, 27–33.

Da Silva-Junior, A.A., De Matos, J.R., Formariz, T.P., Rossanezi, G., Scarpa, M.V., Do Egito, E.S.T., De Oliveira, A.G., 2009. Thermal behavior and stability of biodegradable spray-dried microparticles containing triamcinolone. Int. J. Pharm. 368, 45–55.

Degenring, R.F., Jonas, J.B., 2003. Intravitreal injection of triamcinolone acetonide as treatment for chronic uveitis. Br. J. Ophthalmol. 87, 361.

Duvvuri, S., Majumdar, S., Mitra, A.K., 2003. Drug delivery to the retina: challenges and opportunities. Expert Opin. Biol. Ther. 3, 45–56.

Fang, J.-Y., Fang, C.-L., Liu, C.-H., Su, Y.-H., 2008. Lipid nanoparticles as vehicles for topical psoralen delivery: solid lipid nanoparticles (SLN) versus nanostructured lipid carriers (NLC). Eur. J. Pharm. Biopharm. 70, 633–640.

Feng, S.-S., Huang, G., 2001. Effects of emulsifiers on the controlled release of paclitaxel (Taxol®) from nanospheres of biodegradable polymers. J. Control. Release 71, 53–69.

Freitas, C., Müller, R.H., 1999. Correlation between long-term stability of solid lipid nanoparticles (SLN(TM)) and crystallinity of the lipid phase. Eur. J. Pharm. Biopharm. 47, 125–132.

Hagemann, J., Rothfus, J., 1993. Transitions of saturated monoacid triglycerides: modeling conformational change at glycerol during $\alpha \rightarrow \beta' \rightarrow \beta$ transformation. J. Am. Oil Chem. Soc. 70, 211–217.

Hironaka, K., Inokuchi, Y., Tozuka, Y., Shimazawa, M., Hara, H., Takeuchi, H., 2009. Design and evaluation of a liposomal delivery system targeting the posterior segment of the eye. J Control. Release 136, 247–253.

Hughes, P.M., Olejnik, O., Chang-Lin, J.E., Wilson, C.G., 2005. Topical and systemic drug delivery to the posterior segments. Adv. Drug Deliv. Rev. 57, 2010–2032.

Jannin, V., Pochard, E., Chambin, O., 2006. Influence of poloxamers on the dissolution performance and stability of controlled-release formulations containing Precirol® ATO 5. Int. J. Pharm. 309, 6–15.

Jonas, J., 2005. Intravitreal injection of triamcinolone acetonide. In: Spaide, R.F. (Ed.), Medical Retina. Springer, pp. 143–164.

Jonas, J., 2006. Intravitreal triamcinolone acetonide: a change in a paradigm. Ophthalmic Res. 38, 218–245.

Jonas, J.B., Kreissig, I., Degenring, R., 2005. Intravitreal triamcinolone acetonide for treatment of intraocular proliferative, exudative, and neovascular diseases. Prog. Retin. Eye Res. 24, 587–611.

Kamppeter, B.A., Cej, A., Jonas, J.B., 2008. Intraocular concentration of triamcinolone acetonide after intravitreal injection in the rabbit eye. Ophthalmology 115, 1372–1375.

Kay, J.H., Calandra, J.K., 1962. Interpretation of eye irritation test. J. Soc. Cosmet. Chem. 13, 281–289.

Keck, C.M., Muller, R.H., 2008. Size analysis of submicron particles by laser diffractometry – 90% of the published measurements are false. Int. J. Pharm. 355, 150–163.

Liu, W., Hu, M., Liu, W., Xue, C., Xu, H., Yang, X., 2008. Investigation of the carbopol gel of solid lipid nanoparticles for the transdermal iontophoretic delivery of triamcinolone acetonide acetate. Int. J. Pharm. 364, 135–141.

Mainardes, R.M., Urban, M.C., Cinto, P.O., Khalil, N.M., Chaud, M.V., Evangelista, R.C., Gremiao, M.P., 2005. Colloidal carriers for ophthalmic drug delivery. Curr. Drug Targets 6, 363–371.

Mansoor, S., Kuppermann, B., Kenney, M., 2009. Intraocular sustained-release delivery systems for triamcinolone acetonide. Pharm. Res. 26, 770–784.

Maurice, D.M., 2002. Drug delivery to the posterior segment from drops. Surv. Ophthalmol. 47 (Suppl. 1), S41–S52.

Mclain, V.C., 2008. Safety assessment of poloxamers 101, 105, 108, 122, 123, 124, 181, 182, 183, 184, 185, 188, 212, 215, 217, 231, 234, 235, 237, 238, 282, 284, 288, 331, 333, 334, 335, 338, 401, 402, 403, and 407, poloxamer 105 benzoate, and poloxamer 182 dibenzoate as used in cosmetics. Int. J. Toxicol. 27, 93–128.

Müller, R.H., Lucks, J.S., 1996. Arzneistoffträger aus festen Lipidteilchen, Feste Lipid nanosphären. (SLN). European Patent EP0605497.

Müller, R.H., Mäder, K., Gohla, S., 2000. Solid lipid nanoparticles (SLN) for controlled drug delivery – a review of the state of the art. Eur. J. Pharm. Biopharm. 50, 161–177.

Müller, R.H., Radtke, M., Wissing, S.A., 2002. Solid lipid nanoparticles (SLN) and nanostructured lipid carriers (NLC) in cosmetic and dermatological preparations. Adv. Drug Deliv. Rev. 54, S131–S155.

Nagarwal, R.C., Kant, S., Singh, P.N., Maiti, P., Pandit, J.K., 2009. Polymeric nanoparticulate system: a potential approach for ocular drug delivery. J. Control. Release 136, 2–13.

Piermarocchi, S., Sartore, M., Lo Giudice, G., Maritan, V., Midena, E., Segato, T., 2008. Combination of Photodynamic Therapy and Intraocular Triamcinolone for Exudative Age-Related Macular Degeneration and Long-Term Chorioretinal Macular Atrophy. Arch. Ophthalmol. 126, 1367–1374.

Pretsch, E., Bühlmann, P., Badertscher, M., 2009. IR Spectroscopy. Structure Determination of Organic Compounds. Springer, Berlin Heidelberg, 1–67.

Sahoo, S.K., Dilnawaz, F., Krishnakumar, S., 2008. Nanotechnology in ocular drug delivery. Drug Discov. Today 13, 144–151.

Schoenwald, R.B., Stewart, P., 1980. Effect of particle size on ophthalmic bioavailability of dexamethasone suspensions in rabbits. J. Pharm. Sci. 69, 391–394.

Scott, I.U., Flynn, H.W., Rosenfeld, P.J., 2003. Intravitreal triamcinolone acetonide for idiopathic cystoid macular edema. Am. J. Ophthalmol. 136, 737–739.

Souto, E.B., Müller, R.H., 2006. Investigation of the factors influencing the incorporation of clotrimazole in SLN and NLC prepared by hot high-pressure homogenization. J. Microencapsul. 23, 377–388.

Souto, E.B., Müller, R.H., 2009. Lipid nanoparticles – Effect on bioavailability and pharmacokinetics changes. In: Schäfer-Korting, M. (Ed.), Handbook of Experimental Pharmacology - Novel Drug Delivery Approaches, Vol. 197. Springer Verlag, Heidelberg, Berlin, Germany, pp. 115–142, Chapter 4.

Souto, E.B., Wissing, S.A., Barbosa, C.M., Müller, R.H., 2004. Evaluation of the physical stability of SLN and NLC before and after incorporation into hydrogel formulations. Eur. J. Pharm. Biopharm. 58, 83–90.

Sung, P.P., Jae, K.A., 2008. Changes of aqueous vascular endothelial growth factor and interleukin-6 after intravitreal triamcinolone for branch retinal vein occlusion. Clinical Exp. Ophthalm. 36, 831–835.

Thomas, M.L., Gan, C.M., Polse, K.A., 1997. Sequential staining: the effects of sodium fluorescein, osmolarity, and pH on human corneal epithelium. Optom. Vis. Sci. 74, 207–210.

Tiyaboonchai, W., Tungpradit, W., Plianbangchang, P., 2007. Formulation and characterization of curcuminoids loaded solid lipid nanoparticles. Int. J. Pharm. 337, 299–306.

Valero, J., Egea, M.A., Espina, M., Gamisans, F., Garcia, M.L., 1996. Effect of polymerization coadjuvants on nanocapsule elaboration and triamcinolone acetonide entrapment. Drug Dev. Ind. Pharm. 22, 167–173.

Vivek, K., Reddy, H., Murthy, R., 2007. Investigations of the effect of the lipid matrix on drug entrapment, in vitro release, and physical stability of olanzapine-loaded solid lipid nanoparticles. AAPS Pharm. Sci. Technol. 8, 16–24.

Yang, S.C., Zhu, J.B., 2002. Preparation and characterization of camptothecin solid lipid nanoparticles. Drug Dev. Ind. Pharm. 28, 265–274.

Zhang, J., Fan, Y., Smith, E., 2009. Experimental design for the optimization of lipid nanoparticles. J. Pharm. Sci. 98, 1813–1819.